Fracture Mechanics of Concrete Structures
**Proceedings FRAMCOS-3**
AEDIFICATIO Publishers, D-79104 Freiburg, Germany

# A STUDY ON CONSTITUTIVE THEORY OF ELASTO-PLASTIC ANALYSIS IN FINITE ELEMENT METHOD

J. Ishida
Building Design Dept., Osaka Office, Konoike Construction Co., Ltd.
Osaka, Japan

## Abstract

In this paper a constitutive theory of elasto-plastic analysis using additional loads in Finite Element Method (FEM) is introduced. When a calculated stress set exceeds an assumed yield criterion, an iteration is performed repeatedly with an additional load set until a calculated stress set converges onto the yield criterion surface. Here, this analytical theory is described mainly. In order to verify this theory, some comparisons between analysis and experiment are added. For details, refer to Ishida(1994). As the conclusion, good coincidences between analysis and experiment are observed. Therefore, this analytical theory is thought to be reasonable.
Keywords: elasto-plastic analysis, constitutive theory, yield criterion

## 1 Introduction

The main points of plasticity theory are to decide the criterion in which a material yields and the relation between stress and strain after yield. This paper introduces the latter, i.e. constitutive theory in the yield area.

The constitutive theory described here is the method of giving additional loads for stress to converge onto yield criterion surface. In the theory, the relationship between stress set and yield criterion is visually understandable compared with other conventional theories.

First, an elasto-plastic one-dimensional problem as shown in Fig. 1 will be discussed. Element A and element B are placed parallel and stiffnesses of element A and B are $K_a$= 15 kN/cm and $K_b$= 10 kN/cm respectively. Element B yields at the load of $P_y$ = 20 kN and the applied load is P= 100 kN. $N_a$ and $N_b$ are axial forces in element A and B respectively, and $\delta$ is displacement. This problem can be solved by iteration method as follows.

step 0 : $N_{a\,0} = P \cdot K_a / (K_a+K_b) = 60$
$N_{b\,0} = P \cdot K_b / (K_a+K_b) = 40 > P_y = 20$
$\delta_0 = P / (K_a+K_b) = 4.0$

step 1 : $\Delta P_1^{*1} = N_{b\,0} - P_y = 20$
$N_{a\,1} = (P+\Delta P_1^{*3})K_a / (K_a+K_b) = 72$
$N_{b\,1} = (P+\Delta P_1^{*3})K_b / (K_a+K_b) - \Delta P_1^{*2} = 28 > P_y$ (1)
$\delta_1 = (P+\Delta P_1^{*3}) / (K_a+K_b) = 4.8$
...............

step n : $\Delta P_n = N_{b\,n-1} - P_y$
$N_{a\,n} = (P+\Sigma \Delta P_i)K_a / (K_a+K_b)$
$N_{b\,n} = (P+\Sigma \Delta P_i)K_b / (K_a+K_b) - \Sigma \Delta P_i$
$\delta_n = (P+\Sigma \Delta P_i) / (K_a+K_b)$
...............

This operation is modified Newton-Raphson method. The results are shown in Table 1. This method will be applied for 3-dimensional problems.

Table 1. Results of iteration

| step | Na(kN) | Nb(kN) | ΣΔ Pi(kN) | δ (cm) |
|---|---|---|---|---|
| 0 | 60. | 40. | 0. | 4. |
| 1 | 72. | 28. | 20. | 4.8 |
| 2 | 76.8 | 23.2 | 28. | 5.12 |
| 3 | 78.72 | 21.28 | 31.2 | 5.248 |
| 4 | 79.488 | 20.512 | 32.48 | 5.2992 |
| 5 | 79.7952 | 20.2048 | 32.992 | 5.31968 |
| 6 | 79.9181 | 20.0819 | 33.1968 | 5.32787 |
| 7 | 79.9672 | 20.0328 | 33.2787 | 5.33115 |
| 8 | 79.9869 | 20.0131 | 33.3115 | 5.33246 |
| 9 | 79.9948 | 20.0052 | 33.3246 | 5.33298 |
| 10 | 79.9979 | 20.0021 | 33.3298 | 5.33319 |
| 11 | 79.9992 | 20.0008 | 33.3319 | 5.33328 |
| 12 | 79.9997 | 20.0003 | 33.3328 | 5.33331 |
| 13 | 79.9999 | 20.0001 | 33.3331 | 5.33332 |
| 14 | 80. | 20. | 33.3333 | 5.33333 |

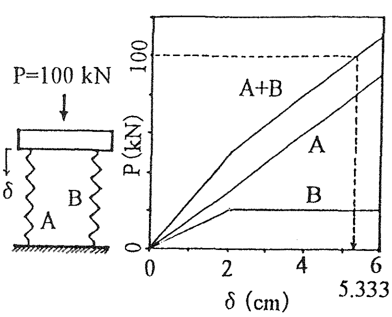


Fig. 1. One-dimensional problem

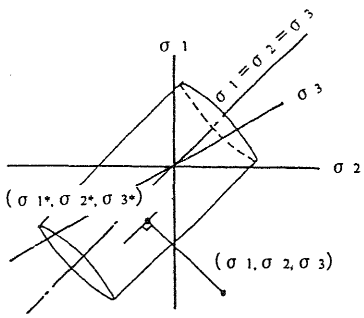


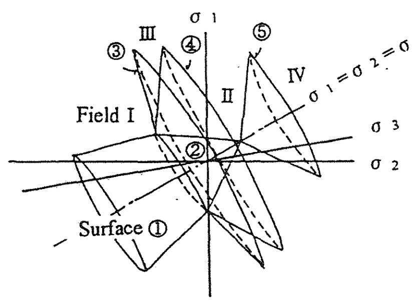


Fig. 2. Yield criterion of steel

Fig. 3. Yield criterion of concrete

At a certain step in incremental load method, calculated principal stress set($\sigma_1, \sigma_2, \sigma_3$) is assumed to exceed yield criterion as shown in Fig.2. The exceeding amount of principal stress set is expressed as ($\Delta\sigma_1, \Delta\sigma_2, \Delta\sigma_3$), which is the difference between ($\sigma_1, \sigma_2, \sigma_3$) and ($\sigma_1^*, \sigma_2^*, \sigma_3^*$). ($\sigma_1^*, \sigma_2^*, \sigma_3^*$) is the point where perpendicular line from ($\sigma_1, \sigma_2, \sigma_3$) intersects the yield criterion surface. Equivalent stress set and equivalent nodal point force set (additional load set) which equilibrate with the excess principal stress set ($\Delta\sigma_1, \Delta\sigma_2, \Delta\sigma_3$) are calculated, then the calculation will be resumed with the external loads in which the additional load sets are added on. The new principal stress set will be obtained from the new stress set, which is a result of subtracting the equivalent stress set from the calculated stress set. The iteration is to be repeated until the principal stress set converge onto the yield criterion surface. The excess principal stress set, the equivalent stress set and the equivalent nodal point force set correspond to $\Delta P_1^{*1}$, $\Delta P_1^{*2}$ and $\Delta P_1^{*3}$ in Eq.(1), respectively. The sign convention is that tension is positive and compression is negative in this paper.

## 2 Analytical theory

### 2.1 Assumption of yield criterion

Fllowing von Mises' criterion, yield criterion for steel is assumed as shown in Fig. 2 and Eq. (2).

$$2\,{}_s f_o{}^2 = (\sigma_1 - \sigma_2)^2 + (\sigma_2 - \sigma_3)^2 + (\sigma_3 - \sigma_1)^2 \qquad (2)$$

where ${}_s f_o$ : yield stress of steel

Yield criterion for concrete is assumed as a composite of two cones as shown in Fig. 3, and Eqs.(3),(4). One cone (Surface ①) has confinement coefficient k and intersection with principal axis at $c f_c$, and the other (Surface ②) has intersections with principal axis at $c f_c$ and $c f_t$. The coefficient k indicates the influence of side stress against tri-axial compression strength of concrete. Surface ③, ④ and ⑤ are surfaces dividing principal stress field. Surface ③ is a cone which is perpendicular to Surface ① at the intersection line of Surface ① and ②. Surface ④ is a cone which is perpendicular to Surface ② at the intersection line of Surface ① and ②. Surface ⑤ is a cone which is perpendicular to Surface ② at the peak. This yield criterion is in a similar form as Drucker-Prager's criterion.

Surface ① $\{\sigma_1+\sigma_2+\sigma_3+3\,cf_c/(k-1)\}^2 = (k+2)^2 C^2/\{2(k-1)^2\}$ (3)

Surface ② $\{\sigma_1+\sigma_2+\sigma_3-2\,cf_t\,cf_c/(cf_t+cf_c)\}^2 = (cf_t-cf_c)^2 C^2/\{2(cf_t+cf_c)^2\}$ (4)

Surface ③ $\{\sigma_1+\sigma_2+\sigma_3-3k\,cf_c/(k+2)\}^2 = 2(k-1)^2 C^2/(k+2)^2$ (5)

Surface ④ $\{\sigma_1+\sigma_2+\sigma_3+(cf_t\,cf_c+3cf_c^2)/(cf_t-cf_c)\}^2 = 2(cf_t+cf_c)^2 C^2/(cf_t-cf_c)^2$ (6)

Surface ⑤ $\{\sigma_1+\sigma_2+\sigma_3-2\,cf_t\,cf_c/(cf_t+cf_c)\}^2 = 2(cf_t+cf_c)^2 C^2/(cf_t-cf_c)^2$ (7)

where $C=\sqrt{(\sigma_1-\sigma_2)^2+(\sigma_2-\sigma_3)^2+(\sigma_3-\sigma_1)^2}$ (8)

$cf_c$ : uni-axial compression strength of concrete ($cf_c < 0$)

$cf_t$ : uni-axial tensile strength of concrete ($cf_t > 0$)

k : confinement coefficient ($k > 1$)

$cf_{c\,max}=cf_c+kp_l$ ($cf_{c\,max}$:tri-axial compression strength,$p_l$:lateral pressure)

### 2.2 Excess principal stress set

For steel, when the principal stress set($\sigma_1,\sigma_2,\sigma_3$) exceeds the yield criterion surface as in Fig.2, the point($\sigma_1^*,\sigma_2^*,\sigma_3^*$) where the perpendicular line from the point($\sigma_1,\sigma_2,\sigma_3$) intersects the yield criterion surface is expressed as Eq.(9). (refer to appendix)

$$\left.\begin{aligned}\sigma_1^*&=(\sigma_1+\sigma_2+\sigma_3)/3+\sqrt{2}\,sf_0(2\sigma_1-\sigma_2-\sigma_3)/(3C)\\ \sigma_2^*&=(\sigma_1+\sigma_2+\sigma_3)/3+\sqrt{2}\,sf_0(2\sigma_2-\sigma_3-\sigma_1)/(3C)\\ \sigma_3^*&=(\sigma_1+\sigma_2+\sigma_3)/3+\sqrt{2}\,sf_0(2\sigma_3-\sigma_1-\sigma_2)/(3C)\end{aligned}\right\} \quad (9)$$

For concrete, when the principal stress set($\sigma_1,\sigma_2,\sigma_3$) exceeds the yield criterion surface (Surface ① , ② as in Fig. 3), the point($\sigma_1^*$, $\sigma_2^*,\sigma_3^*$)is expressed as Eqs.(10)～(13) according to the field which the point($\sigma_1, \sigma_2, \sigma_3$) is located in.

Field I :

$$\left.\begin{array}{l}
\sigma_1^*=B_1\{6cfc/(k+2)^2+\sqrt{2}C/(k+2)-(\sigma_1+\sigma_2+\sigma_3)/(k-1)\} \\
\quad +A_1\{3cfc/(k-1)^2-\sqrt{2}C/(k+2)+(\sigma_1+\sigma_2+\sigma_3)/(k-1)\}(2\sigma_1-\sigma_2-\sigma_3)/C \\
\sigma_2^*=B_1\{6cfc/(k+2)^2+\sqrt{2}C/(k+2)-(\sigma_1+\sigma_2+\sigma_3)/(k-1)\} \\
\quad +A_1\{3cfc/(k-1)^2-\sqrt{2}C/(k+2)+(\sigma_1+\sigma_2+\sigma_3)/(k-1)\}(2\sigma_2-\sigma_3-\sigma_1)/C \\
\sigma_3^*=B_1\{6cfc/(k+2)^2+\sqrt{2}C/(k+2)-(\sigma_1+\sigma_2+\sigma_3)/(k-1)\} \\
\quad +A_1\{3cfc/(k-1)^2-\sqrt{2}C/(k+2)+(\sigma_1+\sigma_2+\sigma_3)/(k-1)\}(2\sigma_3-\sigma_1-\sigma_2)/C
\end{array}\right\} \tag{10}$$

where $A_1=-\sqrt{2}(k+2)(k-1)^2/\{9(k^2+2)\}$, $B_1=-(k+2)^2(k-1)/\{9(k^2+2)\}$

Field II :

$$\left.\begin{array}{l}
\sigma_1^*=B_2\{4cft^2cfc^2/(cft-cfc)^2+\sqrt{2}cftcfcC/(cft-cfc)+cftcfc(\sigma_1+\sigma_2+\sigma_3)/(cft+cfc)\} \\
\quad +A_2\{2cft^2cfc^2/(cft+cfc)^2-\sqrt{2}cftcfcC/(cft-cfc)-cftcfc(\sigma_1+\sigma_2+\sigma_3)/(cft+cfc)\} \\
\quad \cdot(2\sigma_1-\sigma_2-\sigma_3)/C \\
\sigma_2^*=B_2\{4cft^2cfc^2/(cft-cfc)^2+\sqrt{2}cftcfcC/(cft-cfc)+cftcfc(\sigma_1+\sigma_2+\sigma_3)/(cft+cfc)\} \\
\quad +A_2\{2cft^2cfc^2/(cft+cfc)^2-\sqrt{2}cftcfcC/(cft-cfc)-cftcfc(\sigma_1+\sigma_2+\sigma_3)/(cft+cfc)\} \\
\quad \cdot(2\sigma_2-\sigma_3-\sigma_1)/C \\
\sigma_3^*=B_2\{4cft^2cfc^2/(cft-cfc)^2+\sqrt{2}cftcfcC/(cft-cfc)+cftcfc(\sigma_1+\sigma_2+\sigma_3)/(cft+cfc)\} \\
\quad +A_2\{2cft^2cfc^2/(cft+cfc)^2-\sqrt{2}cftcfcC/(cft-cfc)-cftcfc(\sigma_1+\sigma_2+\sigma_3)/(cft+cfc)\} \\
\quad \cdot(2\sigma_3-\sigma_1-\sigma_2)/C
\end{array}\right\} \tag{11}$$

where $A_2 = -\sqrt{2}(cft-cfc)(cft+cfc)^2/\{3cft\,cfc(3cft^2+2cft\,cfc+3cfc^2)\}$,
$B_2= (cft-cfc)^2(cft+cfc)/\{3cft\,cfc(3cft^2+2cft\,cfc+3cfc^2)\}$

Field III :

$$\left.\begin{array}{l}
\sigma_1^* = cfc/3 - \sqrt{2}\,cfc\,(2\sigma_1-\sigma_2-\sigma_3)/(3C) \\
\sigma_2^* = cfc/3 - \sqrt{2}\,cfc\,(2\sigma_2-\sigma_3-\sigma_1)/(3C) \\
\sigma_3^* = cfc/3 - \sqrt{2}\,cfc\,(2\sigma_3-\sigma_1-\sigma_2)/(3C)
\end{array}\right\} \tag{12}$$

Field IV :

$$\sigma_1^* = \sigma_2^* = \sigma_3^* = 2cft\,cfc/\{3(cft+cfc)\} \tag{13}$$

The principal stress set which is exceeding the yield criterion surface, ($\Delta\sigma_1, \Delta\sigma_2, \Delta\sigma_3$) is the difference between those two sets of stress for each case, as expressed as Eq.(14).

$$\left.\begin{array}{l}
\Delta\sigma_1 = \sigma_1-\sigma_1^* \\
\Delta\sigma_2 = \sigma_2-\sigma_2^* \\
\Delta\sigma_3 = \sigma_3-\sigma_3^*
\end{array}\right\} \tag{14}$$

## 2.3 Equivalent stress set and equivalent nodal point force set

The principal stress set is expressed by the stress set as follows.

$$[\sigma_p] = [T]^T [\sigma] [T] \tag{15}$$

where $[\sigma_p]$:principal stress matrix, $[T]$:coordinate transformation matrix
$[\sigma]$ :stress matrix, $[\ ]^T$ :transposed matrix

The equivalent stress set is expressed by the obtained excess principal stress set as follows.

$$[\Delta\sigma] = [T] [\Delta\sigma_p] [T]^T \tag{16}$$

where $[\Delta\sigma]$ :equivalent stress matrix
$[\Delta\sigma_p]$ :excess principal stress matrix

Axial symmetry rectangular ring element is employed for FEM as shown in Fig.4, and the stress set equivalent to the excess principal stress set($\Delta\sigma_1, \Delta\sigma_2, \Delta\sigma_3$) is expressed as follows, developing Eq.(16).

$$\left.\begin{aligned}
\Delta\sigma_r &= \frac{\Delta\sigma_1 + \Delta\sigma_3}{2} + \frac{\Delta\sigma_1 - \Delta\sigma_3}{2}\cos 2\omega \\
\Delta\sigma_z &= \frac{\Delta\sigma_1 + \Delta\sigma_3}{2} - \frac{\Delta\sigma_1 - \Delta\sigma_3}{2}\cos 2\omega \\
\Delta\sigma_\theta &= \Delta\sigma_2 \\
\Delta\tau_{rz} &= \frac{\Delta\sigma_1 - \Delta\sigma_3}{2}\sin 2\omega
\end{aligned}\right\} \tag{17}$$

where $\omega$: an angle between $\sigma_1$ and r-axis

The nodal point force set is expressed by the stress set as follows.

$$\{P\} = \int_V [B]^T \{\sigma\}\, dV \tag{18}$$

where $\{P\}$ :nodal point force vector, $\{\sigma\}$ :stress vector
$[B]$ :strain shape matrix

Developing Eq.(18), the equivalent nodal point force set is obtained as Eq.(19) for the axial symmetry rectangular ring element shown in Fig.4.

$$\{\Delta P\} = \begin{Bmatrix} \Delta p_1 \\ \Delta p_2 \\ \Delta p_3 \\ \Delta p_4 \\ \Delta p_5 \end{Bmatrix} = \begin{bmatrix} -a_1 & a_2 & 0 & -b_1 \\ 0 & 0 & -b_1 & -a_1 \\ a_1 & a_2 & 0 & -b_2 \\ 0 & 0 & -b_2 & a_1 \\ a_1 & a_2 & 0 & b_2 \end{bmatrix} \begin{Bmatrix} \Delta\sigma_r \\ \\ \Delta\sigma_\theta \\ \\ \Delta\sigma_z \end{Bmatrix} \tag{19}$$

$$
\begin{Bmatrix} \Delta p_6 \\ \Delta p_7 \\ \Delta p_8 \end{Bmatrix}
\begin{bmatrix} 0 & 0 & b_2 & a_1 \\ -a_1 & a_2 & 0 & b_1 \\ 0 & 0 & b_1 & -a_1 \end{bmatrix}
\begin{Bmatrix} \\ \Delta \tau_{rz} \\ \\ \end{Bmatrix}
$$

where $\{\Delta P\}$ :equivalent nodal point force vector

$a_1 = (\pi/2)(r_{i+1} + r_i)h$

$a_2 = (\pi/2)(r_{i+1} - r_i)h$

$b_1 = (\pi/3)(r_{i+1} + 2r_i)(r_{i+1} - r_i)$

$b_2 = (\pi/3)(2r_{i+1} + r_i)(r_{i+1} - r_i)$

## 2.4 Application to non-linear materials

The materials which this analytical method can be applied for must be elastic until stress set reaches the yield criterion surface. Non-linear materials such as concrete are considered as overlay models made of some different characteristics whose stress-strain relationships are bi-linear. Yield criterion, as shown in Fig. 3, is then set for each decomposed characteristic. The stress set and the nodal point force set are obtained, and then those are composed.

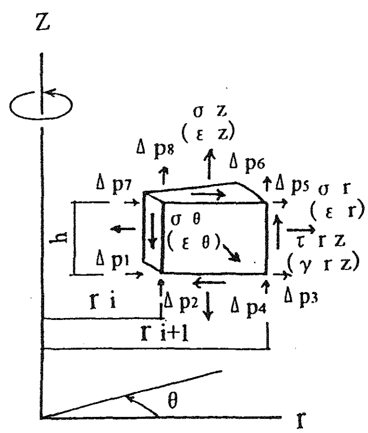


Fig. 4. Ring element for FEM

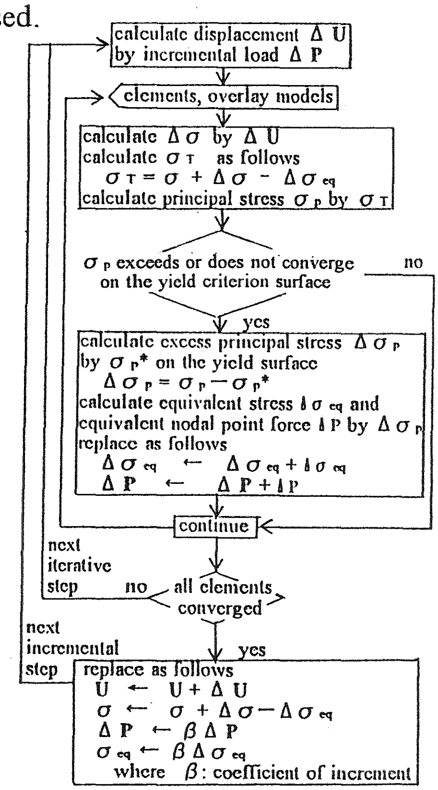


Fig. 5 Flow chart of iteration in incremental method

## 2.5 Flow chart of iteration in incremental load method

A flow chart of iteration in incremental method is shown in Fig. 5, and as show in there the load increment is changeable by coefficient of increment $\beta$.

## 3 The analysis examples

### 3.1 Axial compression test of concrete cylinder specimen

The specifications of concrete used for this analysis are as follows.
size of specimen: 100 mm $\phi \times$ 200 mm, E= 36.2 GPa, $_cf_c$ =− 38.8 MPa, $_cf_t$= 3.88 MPa, $\upsilon$ = 0.17, k = 3

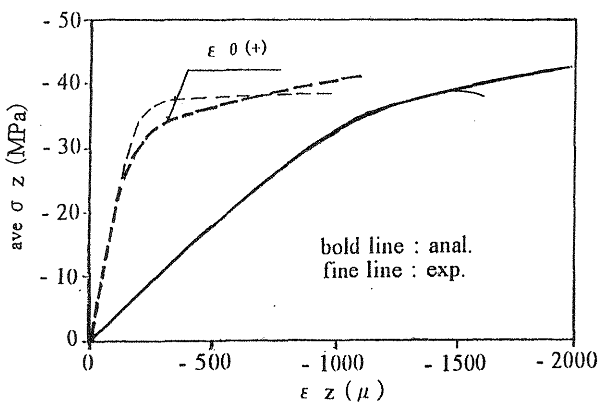


Fig. 6 Stress-strain relationship of concrete

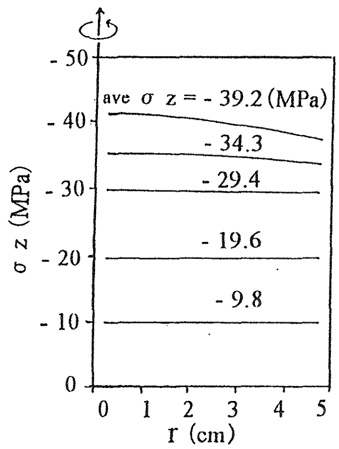


Fig. 7 Distribution of axial stresses of concrete

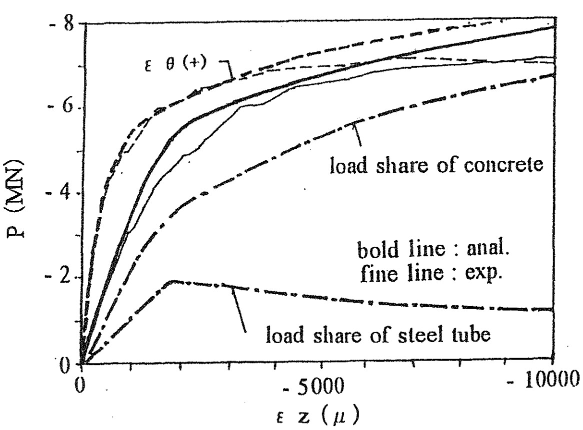


Fig. 8 Load-strain relationship of steel tube

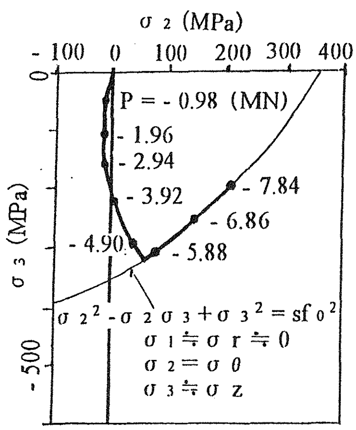


Fig. 9 Stress path of steel tube

In this analysis, the stress-strain relationship of concrete is decomposed to 3 bi-linear models based on the test result. In Fig.6, the stress-strain relationships obtained from analysis are shown along with experimental results. Distributions of axial stress, $\sigma_z$, from analysis are shown in Fig.7. In large load step, the distribution shape comes to resemble a parabola.

### 3.2 Axial compression test of concrete filled steel circular tube

The specifications of steel are as follows. Concrete filled in tube is as shown in the preceding clause.

steel tube: P-318.5 × 6, E= 201 GPa, $_s f_0$ = 358 MPa, $\upsilon$ = 0.3

The load-strain relationships obtained from this analysis are shown in Fig.8 along with experimental results. In this figure, the load shares of concrete and steel tube from analysis are expressed too. In large strain ranges, the increase of load share of concrete is caused by confinement of steel tube. The path of principal stress set ($\sigma_2$, $\sigma_3$) of steel tube from analysis is shown in Fig.9.

## 4 Conclusion

As introduced above, a relatively good coincidence between this analysis and experiment is observed. Therefore, the author is convinced that this analytical theory is reasonable, and expects that this theory will develop in the future.

## 5 References

Ishida, J. (1994) A study on constitutive theory in elasto-plastic analysis using additional load. **J. Struct. Constr. Eng., AIJ,** No. 466, 69-77 (in Japanese)

## Appendix The induction of the intersection point of perpendicular line and yield criterion surface

In Fig. 10, the rotation matrix [ R ] that rotates the space diagonal axis ($\sigma_1 = \sigma_2 = \sigma_3$) around $\sigma_2 = -\sigma_3$ ($\sigma_1 = 0$) axis so as to align it with $\sigma_1$ axis is shown as follows.

$$[R] = \begin{bmatrix} 1/\sqrt{3} & 1/\sqrt{3} & 1/\sqrt{3} \\ -(3+\sqrt{3})/6 & (3-\sqrt{3})/6 & 1/\sqrt{3} \\ (3-\sqrt{3})/6 & -(3+\sqrt{3})/6 & 1/\sqrt{3} \end{bmatrix} \quad (20)$$

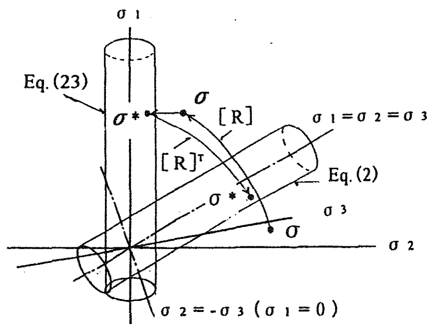


Fig. 10 Transformation of coordinate

Using $[R]$, the point $(\sigma_1, \sigma_2, \sigma_3)$ moves to the point $(\boldsymbol{\sigma}_1, \boldsymbol{\sigma}_2, \boldsymbol{\sigma}_3)$ as shown by the following Eq. (21). Also, the converse is shown by Eq. (22).

$$\{\boldsymbol{\sigma}\} = [R]\{\sigma\} \qquad (21)$$

$$\{\sigma\} = [R]^T \{\boldsymbol{\sigma}\} \qquad (22)$$

By reference, $[R]^T = [R]^{-1}$. Substituting Eq. (22) for $\sigma$ in Eq. (2), we obtain Eq. (23) as follows.

$$2\,sf0^2 / 3 = \boldsymbol{\sigma}_2^2 + \boldsymbol{\sigma}_3^2 \qquad (23)$$

Eq. (23) shows the cylinder where the center axis is $\sigma_1$ axis. The point $(\boldsymbol{\sigma}_1^*, \boldsymbol{\sigma}_2^*, \boldsymbol{\sigma}_3^*)$ where the perpendicular line from the point $(\boldsymbol{\sigma}_1, \boldsymbol{\sigma}_2, \boldsymbol{\sigma}_3)$ intersects this cylinder is expressed as Eq. (24), by elementary geometry.

$$\left.\begin{aligned} \boldsymbol{\sigma}_1^* &= \boldsymbol{\sigma}_1 \\ \boldsymbol{\sigma}_2^* &= \sqrt{2/3}\,sf0\ \boldsymbol{\sigma}_2 / \sqrt{\boldsymbol{\sigma}_2^2 + \boldsymbol{\sigma}_3^2} \\ \boldsymbol{\sigma}_3^* &= \sqrt{2/3}\,sf0\ \boldsymbol{\sigma}_3 / \sqrt{\boldsymbol{\sigma}_2^2 + \boldsymbol{\sigma}_3^2} \end{aligned}\right\} \qquad (24)$$

Substituting Eq. (21) for $\boldsymbol{\sigma}$ in Eq. (24), we can obtain Eq. (25) as follows.

$$\left.\begin{aligned} \boldsymbol{\sigma}_1^* &= (\sigma_1 + \sigma_2 + \sigma_3)/\sqrt{3} \\ \boldsymbol{\sigma}_2^* &= \sqrt{2}\,sf0\ \{-(3+\sqrt{3})\sigma_1 + (3-\sqrt{3})\sigma_2 + 2\sqrt{3}\sigma_3\}/(6C) \\ \boldsymbol{\sigma}_3^* &= \sqrt{2}\,sf0\ \{(3-\sqrt{3})\sigma_1 - (3+\sqrt{3})\sigma_2 + 2\sqrt{3}\sigma_3\}/(6C) \end{aligned}\right\} \qquad (25)$$

Substituting Eq. (25) for $\boldsymbol{\sigma}$ in Eq. (22), we can obtain Eq. (9), described previously. And Eqs. (10)～(13) can be led to by the similar procedure.